Liver Sinusoidal Endothelial Cells Link Hyperinsulinemia to Hepatic Insulin Resistance

Kyoichiro Tsuchiya and Domenico Accili

Insulin signaling in vascular endothelial cells (ECs) is critical to maintain endothelial function but also to mediate insulin action on peripheral glucose disposal. However, gene knockout studies have reached disparate conclusions. Thus, insulin receptor inactivation in ECs does not impair insulin action, whereas inactivation of Irs2 does. Previously, we have shown that endothelial ablation of the three *Foxo* genes protects mice from atherosclerosis. Interestingly, here we show that mice lacking FoxO isoforms in ECs develop hepatic insulin resistance through excessive generation of nitric oxide (NO) that impairs insulin action in hepatocytes via tyrosine nitration of insulin receptors. Coculture experiments demonstrate that NO produced in liver sinusoidal ECs impairs insulin's ability to suppress glucose production in hepatocytes. The effects of liver sinusoidal ECs can be mimicked by NO donors and can be reversed by NO inhibitors in vivo and ex vivo. The findings are consistent with a model in which excessive, rather than reduced, insulin signaling in ECs predisposes to systemic insulin resistance, prompting a reevaluation of current approaches to insulin sensitization. ***Diabetes*** **62:1478–1489, 2013**

Type 2 diabetes is caused by abnormalities of insulin action and β-cell failure (1). Originally identified as a defect of insulin-dependent glucose disposal in skeletal muscle, insulin resistance has gradually morphed into a complex syndrome, under which aspects of impaired lipid metabolism and energy balance and endothelial dysfunction are subsumed (1).

Hyperinsulinemia is the earliest abnormality in the clinical course of insulin resistance and arises as a result of increased secretion and decreased clearance of insulin (2). Insulin is cleared through its own receptor (3). As insulin levels rise to compensate for insulin resistance of target tissues, so does insulin-mediated receptor internalization, followed by receptor degradation (4). As a result, fewer receptors are available at the cell surface to mediate insulin action (5,6). Thus, hyperinsulinemia also begets insulin resistance (7). The phenomenon of insulin-dependent receptor internalization is best documented in liver: insulin concentrations in the portal vein are about fourfold higher than in the hepatic vein owing to receptor-mediated clearance (8). Accordingly, an early consequence of insulin resistance is a reduced number of hepatic insulin receptors (InsRs) (9); conversely, ablating the latter impairs insulin clearance and is sufficient to bring about hyperinsulinemia (10). Less clear is whether receptor downregulation is sufficient to affect insulin action. In fact, the ability of insulin to engender a biological response, such as glucose uptake in adipocytes or inhibition of glucose production in liver, levels off at hormone concentrations that are associated with minimal receptor occupancy (<10%) (5,6,11). Herein lies a pathophysiological conundrum that has never been satisfactorily addressed even as it might hold the key to unraveling this critical clinical problem.

In considering the systemic effects of hyperinsulinemia, one has to be mindful that the cell type most likely to bear the brunt of this pathophysiologic abnormality is the vascular endothelial cell (EC). The literature is rife with reports of abnormal endothelial function secondary to insulin resistance in vascular endothelium (12–15). And tracer studies have documented in detail that insulin diffusion across the endothelial barrier is a factor in determining insulin sensitivity (16,17). But the metabolic effects of mutations affecting insulin sensitivity in ECs are heterogeneous. Thus, InsR ablation has no detectable effect on insulin sensitivity (14), while Irs2 ablation impairs insulin-dependent glucose uptake in muscle (12). These differences might be due to the fact that, unlike most peripheral target tissues of insulin action, a majority of InsRs in ECs are engaged in heterodimer formation with IGF1 receptors (18) that might limit their affinity to bind insulin (19).

To address the question of whether endothelial insulin signaling modulates insulin sensitivity, we took a gain-of-function approach. FoxO proteins are negative regulators of insulin signaling. As a result, ablation of the three *Foxo* genes in vascular ECs (Vascular EC triple Foxo KnockOut [*VECKO*]) increases the biological actions of insulin in this cell type and protects $Ldlr^{-/-}$ mice from atherosclerosis (20). Thus, we used *VECKO* mice to investigate the role of endothelial insulin signaling in modulating peripheral insulin action.

RESEARCH DESIGN AND METHODS

We have described vascular EC-specific triple FoxO knockout (*VECKO*) mice (20). We used only male mice for experiments. We infused insulin (or PBS as control) for 72 h using an Alzet 1003D osmotic pump. We measured body composition by NMR (Bruker Optics), blood glucose with glucometer (One Touch Ultra; Lifescan), plasma insulin (Mercodia), C-peptide (Millipore) by ELISA, and triglyceride (Cayman chemical), cholesterol, and nonesterified fatty acids by colorimetric assays (Cholesterol E and NEFA C; Wako Pure Chemicals). We have previously described the procedure for intraperitoneal glucose (2 g · kg^{-1}), pyruvate (2 g · kg^{-1}), and insulin (0.75 units · kg^{-1}) tolerance tests (21). Mice are maintained with standard or high-fat (60% of calories from fat; Research Diets) diet for indicated periods. The Columbia University Animal Care and Utilization Committee approved all procedures.

Cell culture and coculture. For liver sinusoidal ECs (LSECs), we minced livers, which were then incubated for 1 h at 37°C in Dulbecco's modified Eagle's medium (DMEM) containing 0.2% collagenase type 1 (Worthington), DNaseI (Sigma), and 0.25% BSA. We resuspended digested tissue with DMEM

From the Naomi Berrie Diabetes Center and Department of Medicine, College of Physicians and Surgeons, Columbia University, New York, New York.
Corresponding author: Domenico Accili, da230@columbia.edu.
Received 20 September 2012 and accepted 14 December 2012.
DOI: 10.2337/db12-1296
This article contains Supplementary Data online at http://diabetes.diabetesjournals.org/lookup/suppl/doi:10.2337/db12-1296/-/DC1.

See accompanying commentary, p. 1386.

containing 5% horse serum and centrifuged at 50*g* for 3 min. Supernatant was centrifuged at 400*g* for 5 min. The pellets were resuspended in 0.3 mL magnetic-activated cell sorting buffer, and CD146 microbeads (Miltenyi Biotec) were added, mixed, and incubated for 30 min at 4°C. LSEC purified by magnetic-activated cell sorting column were plated and cultured with DMEM with 5% horse serum, nonessential amino acids, 0.2 mg/mL heparin, 0.1 mg/mL endothelial mitogen (Biomedical Technologies), 10 ng/mL vascular endothelial growth factor, 10 ng/mL epidermal growth factor, 100 units/mL penicillin, and 0.1 mg/mL streptomycin. Cells were used after serum starvation for 18 h. Primary mouse hepatocytes were isolated from 8-week-old male mice and cultured with DMEM containing 0.25% BSA for 18 h before experiments as previously described (22). For coculture, we plated isolated LSEC onto cell culture inserts (BD) at a density of 1.0×10^5 cells/cm^2 and cultured them with DMEM containing 5% horse serum for 4 h. After washing cells with PBS six times, we transferred cell culture inserts above primary hepatocytes in multiwell plates and cultured with DMEM containing 0.25% BSA for an additional 18 h.

Immunocytochemistry. We performed FoxO1 immunocytochemistry as previously described (23) with fluorescein isothiocyanate–conjugated anti-rabbit IgG (Jackson ImmunoResearch) as secondary antibody. We fixed liver specimens in 10% buffered formalin for histological analysis and stained using hematoxylin-eosin or nitrotyrosine.

Nitric oxide production. We loaded LSEC cultures with diaminofluorescein-2 diacetate (DAF-2 DA) (0.5 μmol/L; Invitrogen) for 30 min at 37°C, washed three times with DMEM, and incubated them in the dark. We used fluorescent microscopy to score cells, followed by ImageJ analysis. We assayed nitrite levels using Greiss (Enzo).

cGMP measurement. Frozen liver tissue (100–200 mg) was precipitated in 5% trichloroacetic acid at 4°C and centrifuged at 1,000*g* for 10 min. The supernatant was extracted with ether saturated with water. cGMP concentration was measured by enzyme immunoassay (Cayman chemical). The amount of cGMP was normalized to tissue weight.

Glucose production. We treated primary mouse hepatocytes with a combination of dexamethasone (500 nmol/L) and cAMP (100 nmol/L) for 4 h and then incubated them for 6 h in glucose production buffer (glucose-free DMEM, pH 7.4, containing 30 mmol/L sodium lactate and 3 mmol/L sodium pyruvate without phenol red) with dexamethasone/cAMP in the presence or absence of insulin (10 nmol/L) and/or DETA-NONOate (2 mmol/L). At the end of the incubation, we aspirated 0.1 mL medium to measure glucose using a glucose oxidase assay (Sigma). Total protein concentration was measured to correct for cell count.

mRNA analysis. We extracted RNA using TRIzol (Invitrogen), synthesized cDNA with a High Capacity cDNA Reverse Transcription kit (Applied Biosystems), and performed quantitative RT-PCR using a GoTaq SYBR Green qPCR kit (Promega) in a Chromo4 Real-Time PCR Detection system (Bio-Rad). Primer sequences are available on request.

Protein analysis. Tissues or cells were lysed by buffer containing 2% SDS, 50 mmol/L Tris-HCl, and 5 mmol/L EDTA. For immunoprecipitation, we lysed liver or cells in radioimmunoprecipitation assay buffer with protease/phosphatase inhibitors. The lysates were subjected to immunoprecipitation with 5 μg anti–InsR-β antibody. Immunoblotting was performed followed by enhanced chemiluminescence detection (GE Lifescience).

Statistical analysis. We performed comparisons using paired or unpaired *t* test with appropriate Bonferroni post hoc corrections. We present results as means ± SEM or 95% CI as appropriate. We used the customary threshold $P < 0.05$ to declare statistical significance.

RESULTS

Constitutive insulin signaling in ECs and hepatic insulin resistance. When *VECKO* mice are studied in the background of *Ldlr*$^{-/-}$ mice and fed a Western-type diet, they show the same insulin sensitivity as *Ldlr*$^{-/-}$ controls (20). However, this might be due to the combined effects of *Ldlr* mutation and diet trumping the effect of the *Foxo* mutations. To address this question, we studied *VECKO* mice fed a standard diet (SD). Surprisingly, we observed impaired glucose tolerance and decreased insulin sensitivity in *VECKO* mice, independent of body weight and composition (Fig. 1*A–E*). Pyruvate tolerance tests were consistent with increased hepatic glucose output (Fig. 1*F* and *G*). *VECKO* mice also showed higher fed glucose, insulin, C-peptide, and cholesterol, as well as fasting cholesterol and triglycerides, than wild-type (WT) mice (Fig. 1*H–N*). To assess insulin sensitivity, we analyzed insulin signaling in liver, fat, and skeletal muscle after portal administration of an insulin bolus. In liver of *VECKO* mice, insulin-induced InsR and Irs1 phosphorylation was attenuated (Fig. 2*A* and Supplementary Fig. 1*A*), as was Akt phosphorylation on S473 and T308. Consequently, insulin-induced glycogen synthase kinase (Gsk) 3β, extracellular signal–related kinase (Erk), and FoxO1/3a phosphorylation were decreased. In contrast, insulin-induced Akt and Gsk3β phosphorylation were comparable in adipose and muscle (Supplementary Fig. 1*B* and *C*).

We also analyzed changes in liver insulin signaling in response to fasting and refeeding. Phosphorylation of InsR, Pdk1, and Akt (T308) was decreased in refed *VECKO* mice compared with control littermates (Fig. 2*B* and Supplementary Fig. 1*D*) and was associated with increased protein and mRNA levels of glucose-6-phosphatase (Fig. 2*B* and *C* and Supplementary Fig. 1*D*). Refeeding-induced changes of *Irs2*, *Pck1*, *Igfbp1*, and *Gck* were also attenuated (Fig. 2*D–G*), and glycogen levels were reduced (Fig. 2*H* and *I*). In contrast, there were no differences in hepatic triglyceride content between fasted control and *VECKO* mice (data not shown). These data indicate that *VECKO* mice have hepatic insulin resistance. SD-fed *VECKO* mice did not show liver, pancreas, or kidney dysfunction by serum chemistry (data not shown).

Analyses of insulin signaling in isolated hepatocytes versus sinusoidal ECs. The liver is composed of ~80% hepatocytes and ~20% other cell types that include LSECs, Kupffer, stellate, ductal, and smooth muscle cells. We wished to determine whether the observed decrease in insulin signaling originated in hepatocytes versus LSEC or other cell types. To this end, we isolated hepatocytes, LSECs, and other cell types using immunoabsorption with anti-CD146 antibodies. Eluted cells demonstrated typical morphology and acLDL uptake (Supplementary Fig. 2*A* and *B*), as well as a near-complete absence of FoxO1 and 3a protein and mRNA (20) (Supplementary Fig. 2*C* and *D*).

Immunoblotting of eluate and flow through from CD146 immunoabsorption fractions revealed that proteins required for insulin signaling—InsR, Irs and Akt—are enriched ~20- and 50-fold in hepatocytes compared with LSECs and other cells, respectively (Fig. 3*A*). In contrast, Erk and endothelial nitric oxide (NO) synthase (eNos) are enriched ~50-fold in LSECs compared with other cell types. Given that insulin signaling is decreased by ~40% in *VECKO* mice, the impairment must largely occur in hepatocytes. In primary hepatocytes, InsR and Akt phosphorylation were comparable between control and *VECKO* mice, suggesting that a non–hepatocyte-autonomous mechanism induced insulin resistance in *VECKO* mice liver (Fig. 3*B*).

Increased NO production in LSECs from VECKO mice. In primary LSEC cultures from *VECKO* mice, we observed a stark increase of eNos protein levels and phosphorylation at the Akt-dependent site, Ser1176 (24). In fact, unlike control LSEC—in which phosphorylated (p) Ser1176 was only detected after insulin stimulation—*VECKO* LSECs showed increased basal levels of pSer1176 eNos that could not be further stimulated by insulin (Fig. 3*C* and *D* and Supplementary Fig. 2*E–G*). These data are consistent with prior work indicating that FoxOs suppress eNos expression (20,25,26). Consistent with these findings, *Nos3* mRNA levels were markedly increased, whereas—unlike aortic ECs from *VECKO* mice (20)—*Nos2* levels were normal (Fig. 3*C*). These data indicate that eNos is

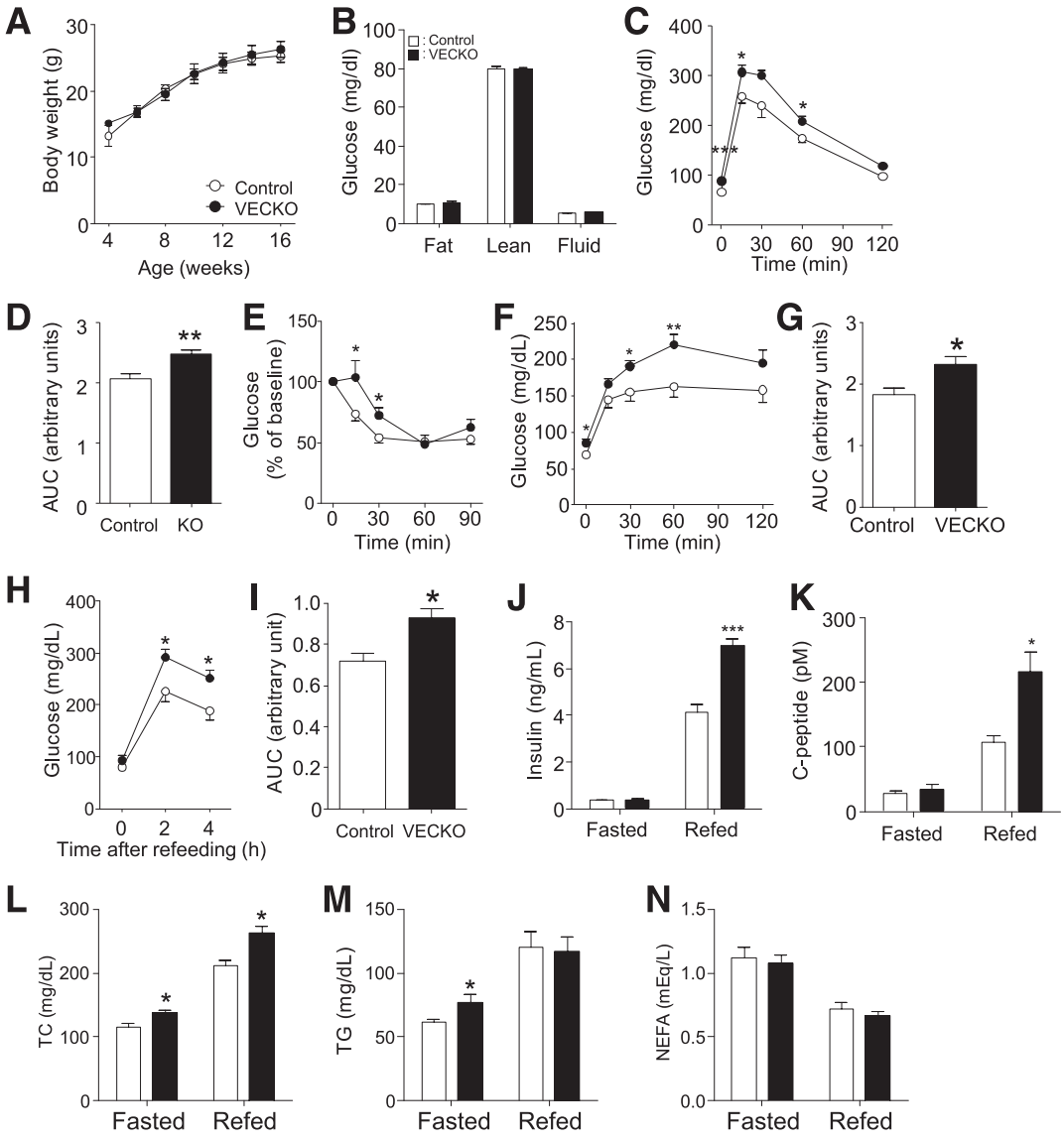

FIG. 1. Metabolic characterization of SD-fed mice. Body weight (*A*) and body composition (*B*) in 12-week-old SD-fed WT and *VECKO* mice (n = 8–10). Intraperitoneal glucose tolerance tests (*C*) and area under curve (AUC) (*D*) in 11-week-old SD-fed WT and *VECKO* mice after an 18-h fast (n = 7–10). *E*: Intraperitoneal insulin tolerance tests in 12-week-old mice after 2-h fast (n = 5–7). Glucose levels (*F*) and area under the curve (*G*) in pyruvate tolerance tests after 18-h fast. Glucose (*H*), area under the curve (*I*), insulin (*J*), C-peptide (*K*), total cholesterol (TC) (*L*), triglyceride (TG) (*M*), and nonesterified fatty acid (NEFA) (*N*) levels in 13-week-old mice fed an SD and fasted for 16 h without refeeding (0 h, fasted) or fasted for 16 h and then refed for 4 h (refed) (n = 5–7). *P < 0.05, **P < 0.01, ***P < 0.001 vs. WT.

persistently activated in LSECs from *VECKO* mice, irrespective of insulin stimulation, and confirm the robustness of *VECKO* mice as a model of constitutive endothelial insulin signaling.

We further determined concentrations of NO metabolites (nitrate/nitrite) in conditioned media of LSEC and in liver. We found that NO metabolites increased in both experimental systems and were normalized by pretreatment with the eNos inhibitor, L-NG-nitroarginine methyl ester (L-NAME) (Fig. 3*E* and *F*). Liver cGMP was increased in *VECKO* mice and was normalized by L-NAME treatment (Fig. 3*G*). Likewise, basal and insulin-stimulated NO production were enhanced in LSECs from *VECKO* mice and blunted by L-NAME pretreatment (Fig. 3*H*). These data indicate that there is increased eNos-dependent NO production in *VECKO* LSECs.

Coculture with LSECs impairs hepatocyte insulin signaling. The findings of *1*) impaired hepatic insulin signaling in spite of *2*) preserved signaling in isolated primary hepatocytes and *3*) increased NO production in LSECs suggest the working hypothesis that NO released by FoxO-deficient LSECs impairs insulin signaling in vivo, contributing to the pathogenesis of hepatic insulin resistance. To test this hypothesis, we first conducted reconstitution experiments in which we cocultured primary hepatocytes with LSEC from *VECKO* mice, using transwell chambers with gas-permeable bottoms. Coculturing impaired insulin-induced phosphorylation of InsR and Akt (Ser473) (Fig. 4*A*). The impairment was partially reversed by pretreatment with the eNos inhibitor, L-NAME, consistent with its being mediated by LSEC-released NO. We obtained similar data using cocultures of hepatocytes with WT LSECs (Supplementary Fig. 3*A*–*D*).

Next, we compared the effect of coculturing primary hepatocytes with LSECs derived either from WT or from *VECKO* mice on insulin regulation of gene expression. Addition of dexamethasone and cAMP increased expression

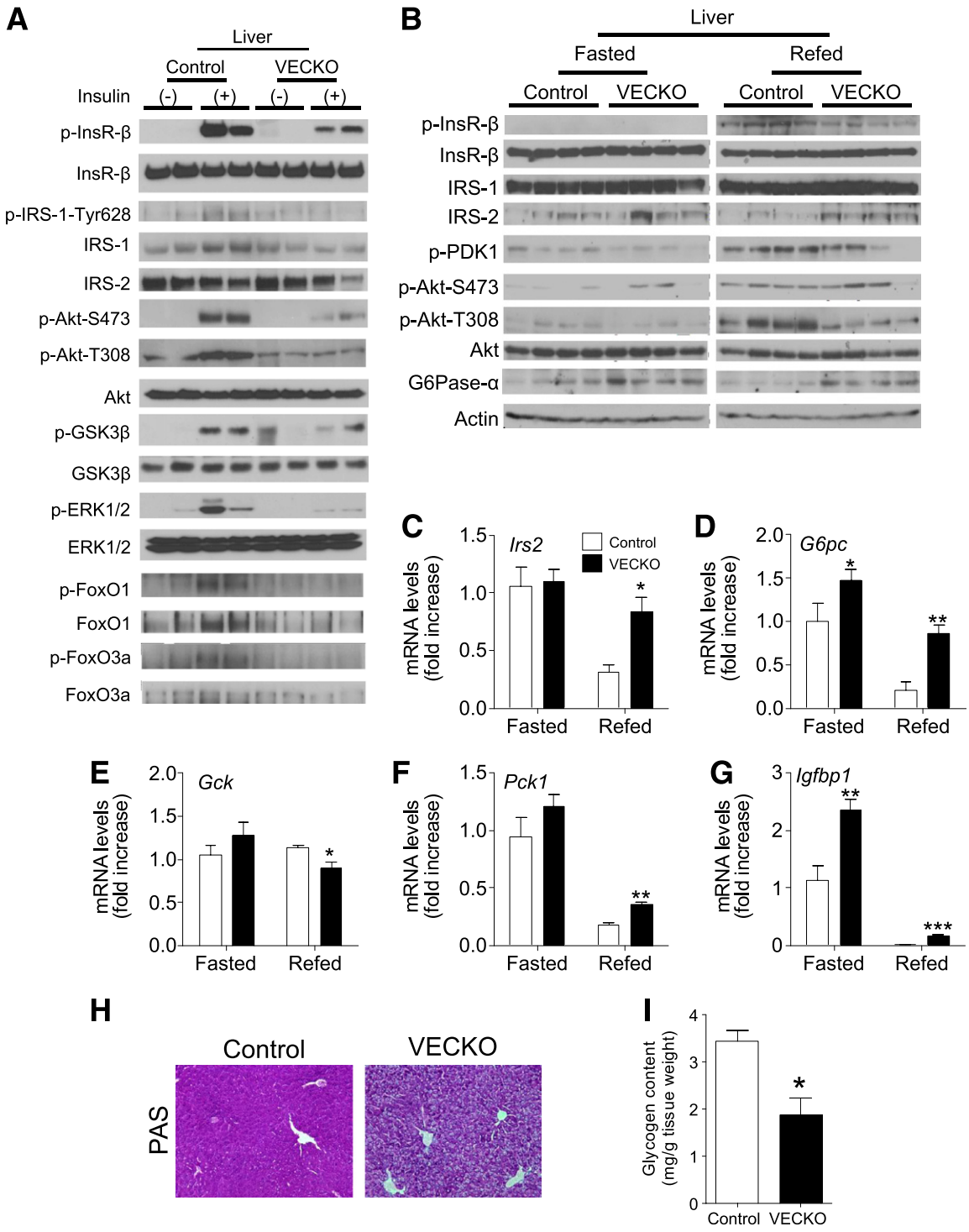

FIG. 2. Insulin-induced hepatic signaling pathways in SD-fed mice. *A*: Immunoblots of liver insulin signaling after insulin injection in 11-week-old WT and *VECKO* mice fed an SD. After 16-h fast, mice were injected with insulin (5 mU/g body wt) or PBS and livers were collected 3 min later (n = 3–4). Immunoblots of liver insulin signaling (*B*) and gene expression (*C–G*) in 12-week-old WT and *VECKO* mice fed an SD and fasted for 16 h without refeeding (fasted) or fasted for 16 h and then refed for 4 h (refed) (n = 4–6). Representative liver PAS staining (*H*) and glycogen content (*I*) in refed mice (n = 4). PDK, phosphoinositide-dependent kinase. *P < 0.05, **P < 0.01, ***P < 0.001 vs. WT. G6Pase-α, glucose-6-phosphatase-α. (A high-quality color representation of this figure is available in the online issue.)

of *G6pc*, *Pck1*, *Pgc1α*, and *Igfbp1* to varying degrees. Coculture with WT LSECs partly prevented insulin inhibition of dexamethasone/cAMP-induced *G6pc* and *Pck1* expression, with a more limited effect on *Igfbp1* (Fig. 4*B–E*). We saw no effect on *Pgc1α* expression (Fig. 4*D*). Coculture with LSECs from *VECKO* mice had a greater inhibitory effect on the ability of insulin to regulate *G6pc* and *Pck1* than WT LSEC (Fig. 4*B* and *C*). These data indicate that LSECs physiologically counteract insulin signaling and that FoxO ablation in LSECs—possibly acting through increased NO production—further impairs insulin action in hepatocytes.

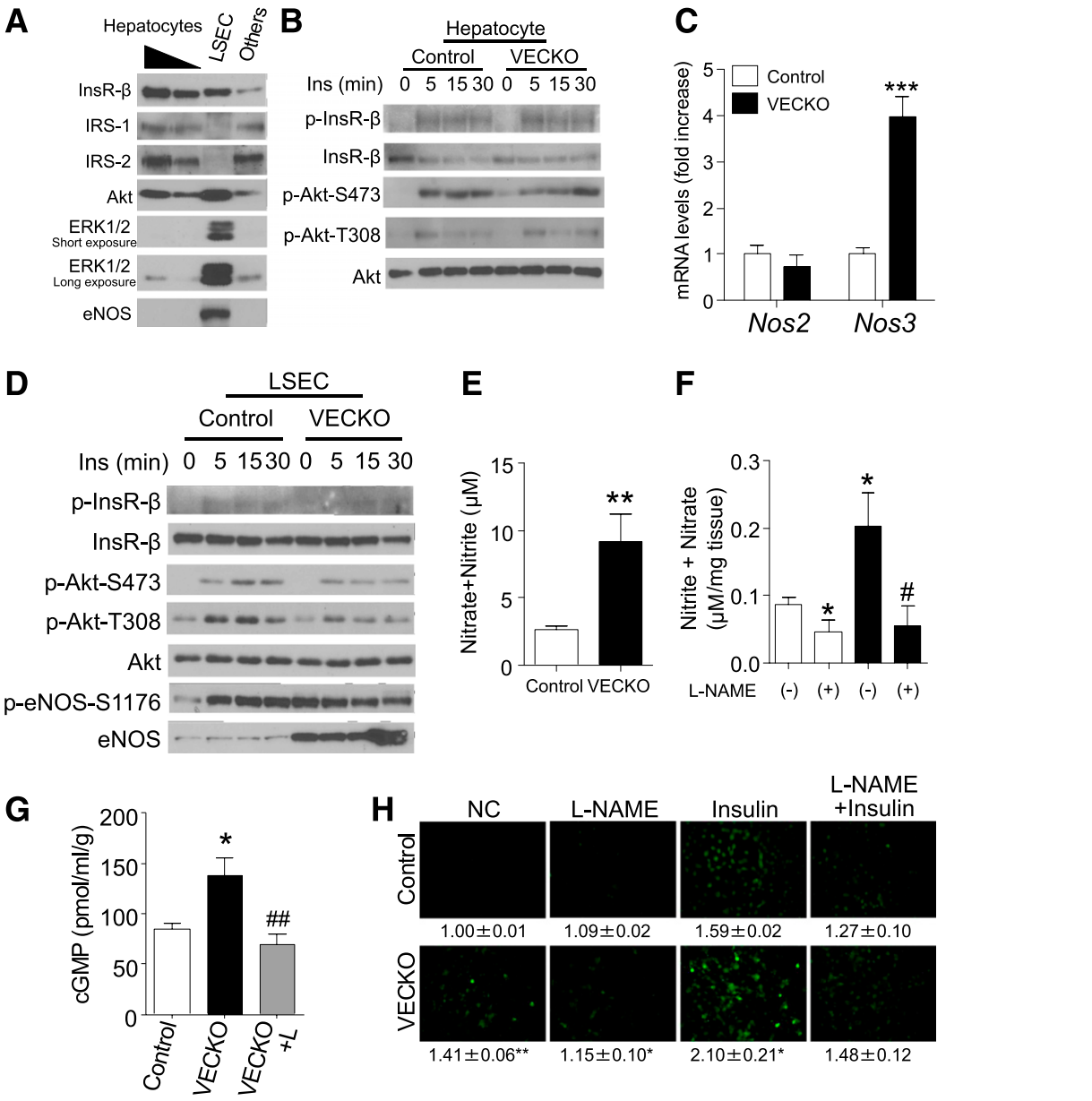

FIG. 3. eNos expression and NO production in LSECs. ***A*: Representative immunoblots of insulin (Ins) signaling and eNos in hepatocytes (1 of 200 or 1 of 100 of total amount), LSECs, and other cellular fractions in liver. A part of liver in a WT mouse was digested with collagenase and was fractionated as described in RESEARCH DESIGN AND METHODS. *B*: Immunoblots of insulin signaling in primary hepatocytes isolated from WT and *VECKO* mice. *C*: *Nos2* and *Nos3* mRNA levels in cultured LSECs from WT and *VECKO* mice. *D*: Representative immunoblots of insulin signaling and p- and total eNos in cultured LSECs from WT and *VECKO* mice after insulin treatment. Nitrate/nitrite concentration in media after 24-h culture of LSEC (*E*) or 4-h incubation of resected liver (*F*) with or without L-NAME pretreatment ($n = 4$). *G*: cGMP content of liver from control and *VECKO* mice with or without L-NAME (L) treatment. L-NAME administration and fasting were started from 16 h prior to analysis ($n = 5$). *H*: Insulin-stimulated NO production visualized by DAF-2 DA fluorescence and quantification in cultured LSECs from WT and *VECKO* mice pretreated with or without L-NAME (1 mmol/L). The numbers indicate arbitrary units of fluorescence intensity (fold increase) ($n = 4$). **P* < 0.05, ***P* < 0.01, ****P* < 0.001 vs. WT. NC, nonstimulated control. #*P* < 0.05, ##*P* < 0.01 vs. *VECKO* without L-NAME treatment. (A high-quality color representation of this figure is available in the online issue.)**

To test the hypothesis that excessive NO production affected hepatic insulin sensitivity in vivo, we performed glucose and insulin tolerance tests in C57Bl6 mice after administering the NO donor, DETA-NONOate. DETA-NONOate increased glucose levels, caused glucose intolerance and insulin resistance (Fig. 4*F* and *G*), and increased G6pc protein and mRNA (Fig. 4*H* and *I*). This compound also increased expression of gluconeogenic genes and G6pc protein in primary hepatocytes. The effects were preempted by pretreatment with the guanylate cyclase inhibitor, ODQ (Supplementary Fig. 4*A* and *B*). The cGMP analog, 8-Br-cGMP, also increased gluconeogenic genes in primary hepatocytes, suggesting that NO induces gluconeogenic genes in a guanylate cyclase/cGMP–dependent manner. Moreover, the ability of insulin to suppress dexamethasone/cAMP induction of gluconeogenic genes (*G6pc* and *Pck1*) as well as glucose production in primary hepatocytes was significantly blunted by DETA-NONOate treatment (Fig. 4*J* and *K*). These data indicate that exogenous NO blunts the ability of insulin to suppress glucose production via regulating gluconeogenic gene expression.

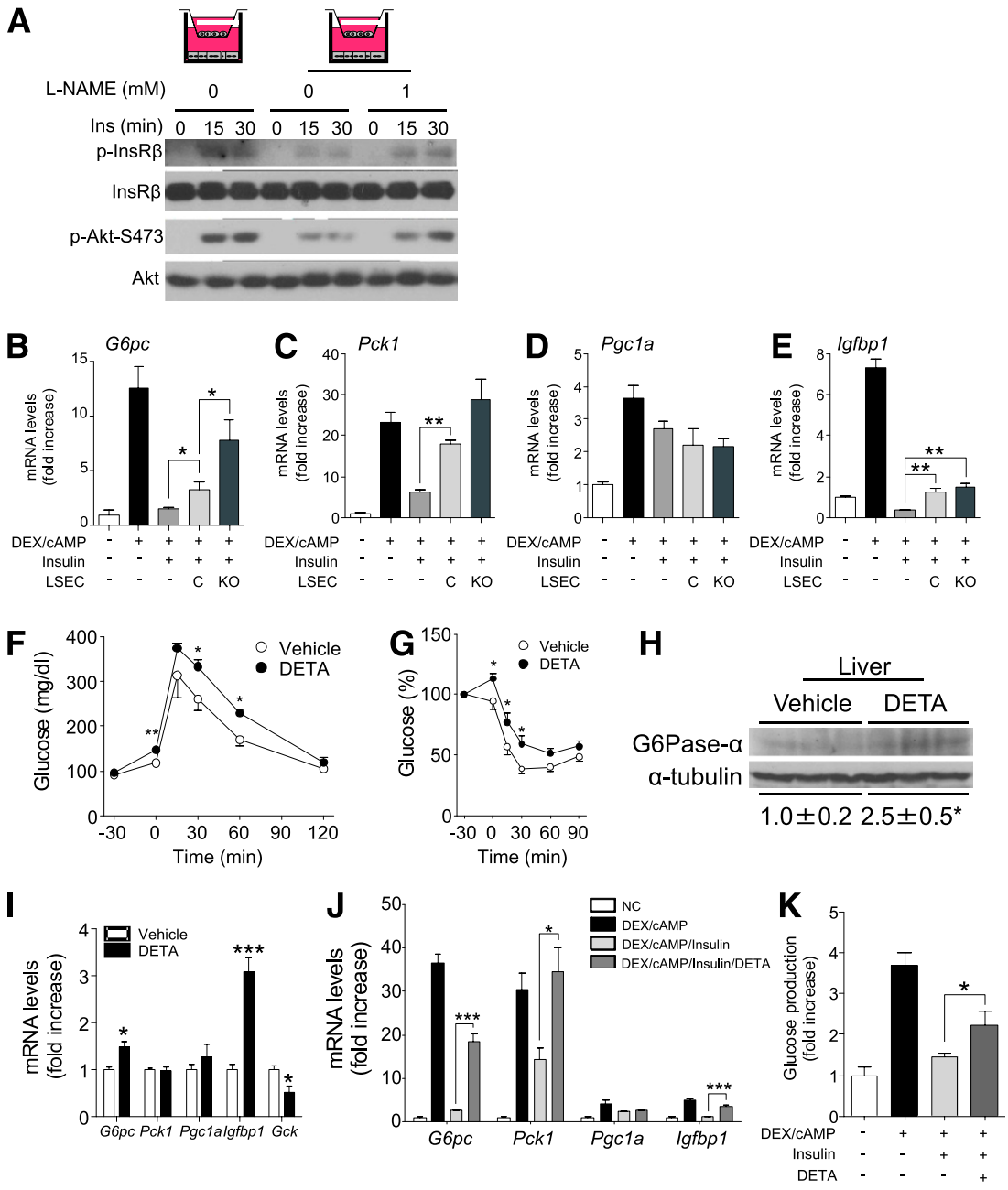

FIG. 4. Glucose tolerance and glucose production in NO-treated mice and hepatocytes. *A*: Representative immunoblots of insulin-stimulated primary hepatocytes cocultured with LSECs from WT or *VECKO* mice in transwell systems. Primary hepatocytes and LSECs were cultured in transwell systems with or without L-NAME (1 mmol/L) for 18 h. Hepatocytes and LSECs were stimulated with insulin (Ins) (10 nmol/L) for indicated times (n = 4). *B–E*: Gluconeogenic gene expression in primary hepatocytes cultured with LSECs from WT or *VECKO* mice in transwell systems (n = 4). Intraperitoneal glucose (*F*) and insulin (*G*) tolerance in 8-week-old SD-fed C57Bl6 mice injected with DETA-NONOate (DETA) or vehicle 30 min prior (−30 min) to glucose or insulin (n = 5) injection. Liver G6pc protein (*H*) and gluconeogenic gene expression (*I*) in C57Bl6 mice after 30 min of DETA-NONOate (20 mg/kg body wt i.p.) or vehicle injection (n = 3). *J*: Gluconeogenic gene expression in primary hepatocytes treated with or without DETA-NONOate. Primary hepatocytes were stimulated with dexamethasone (DEX)/cAMP for 8 h. DETA-NONOate (2.5 mmol/L) and/or insulin (10 nmol/L) were added after 2 and 4 h of DEX/cAMP stimulation, respectively (n = 4). *K*: Glucose production in primary hepatocytes treated with or without DETA-NONOate. Primary hepatocytes stimulated with DEX/cAMP in glucose production buffer for 4 h were stimulated with insulin or insulin/DETA-NONOate (2.5 mmol/L) for an additional 6 h. (n = 4). *P < 0.05, **P < 0.01, ***P < 0.001 vs. vehicle or between indicated groups. G6Pase-α, glucose-6-phosphatase-α. (A high-quality color representation of this figure is available in the online issue.)

LSEC-derived NO promotes tyrosine nitration of hepatocyte InsR. How does NO produced in LSECs affect insulin signaling in hepatocytes? When NO production exceeds its degradation in the presence of highly reactive oxygen, it gives rise to peroxynitrite that can promote nitration of tyrosine residues on proteins (27). Indeed, treatment of primary hepatocytes with DETA-NONOate caused tyrosine nitration of InsR (Supplementary Fig. 5). Tyrosine nitration of InsR impairs their insulin-induced tyrosine phosphorylation and results in insulin resistance (28). Immunoblotting demonstrated a generalized increase of protein tyrosine nitration in livers of *VECKO* mice, whereas there was no difference in protein *S*-nitrosylation (Fig. 5*A–C*). In addition, immunoblotting with nitrotyrosine antibodies of InsR immunoprecipitates showed an increased tyrosine nitration of InsRs in *VECKO* liver (Fig.

5*D*). Immunohistochemistry of liver sections with anti-nitrotyrosine antibodies also showed increased immunoreactivity in *VECKO* liver (Fig. 5*E*). These data indicate that tyrosine nitration of InsR, possibly caused by excessive NO from LSECs, is associated with hepatic insulin resistance in *VECKO* mice.

Hyperinsulinemia increases NO production in LSECs. The findings show that constitutive insulin signaling—as brought about by FoxO ablation—can promote NO-dependent hepatic insulin resistance. But do common forms of hyperinsulinemia result in constitutive endothelial insulin signaling? To address this question, first we examined the effect of chronic insulin treatment using LSEC cultures preincubated with insulin for 24 h. This treatment reduced InsR expression and Akt phosphorylation without impairing FoxO1/3a phosphorylation (Fig. 6*A*). Accordingly, chronic insulin treatment increased FoxO1 nuclear exclusion, NO production (Fig. 6*B–D*), eNos, and *Nos3* expression (Fig. 6*C*) in a phosphatidylinositol 3-kinase–dependent manner (Fig. 6*B–E*). These data are consistent with previous findings in 3T3-L1 cells (29) and demonstrate that FoxO remains sensitive to insulin inhibition even under conditions that impair Akt phosphorylation. Next, we administered insulin to C57BL6 mice using an osmotic minipump for 72 h and compared insulin signaling in liver with PBS-infused mice. Insulin treatment elevated serum insulin levels by approximately threefold (Fig. 6*F*) and, similar to LSECs, it decreased Akt phosphorylation but not FoxO phosphorylation (Fig. 6*G–J*). These data indicate that chronic hyperinsulinemia uncouples Akt phosphorylation from FoxO inhibition and are consistent with the possibility that hyperinsulinemia leads to eNos-dependent NO production in LSECs.

eNos inhibition prevents high-fat diet–induced insulin resistance and liver protein nitration in VECKO mice. High-fat diet (HFD) causes insulin resistance with hyperinsulinemia (30). Therefore, we sought further confirmation of our working model by treating HFD-fed C57BL6 mice with L-NAME. Body weight increased after 5 days on HFD and was not affected by L-NAME treatment (Fig. 7*A*). Since liver inducible NO synthase (iNos) levels did not change under these conditions (data not shown), we propose that L-NAME treatment worked as a bona fide eNOS inhibitor. Glucose tolerance tests showed that L-NAME treatment normalized HFD-induced glucose intolerance (Fig. 7*B*) and fasting hyperglycemia (Fig. 7*C*). Fasting insulin levels tended to improve in L-NAME–treated HFD mice (Fig. 7*D*). L-NAME treatment also decreased fasting serum cholesterol (Supplementary Fig. 6*A*). As shown in the experiments with chronic insulin administration, 5-day HFD decreased Akt phosphorylation but was associated with increased FoxO phosphorylation (Fig. 7*E* and

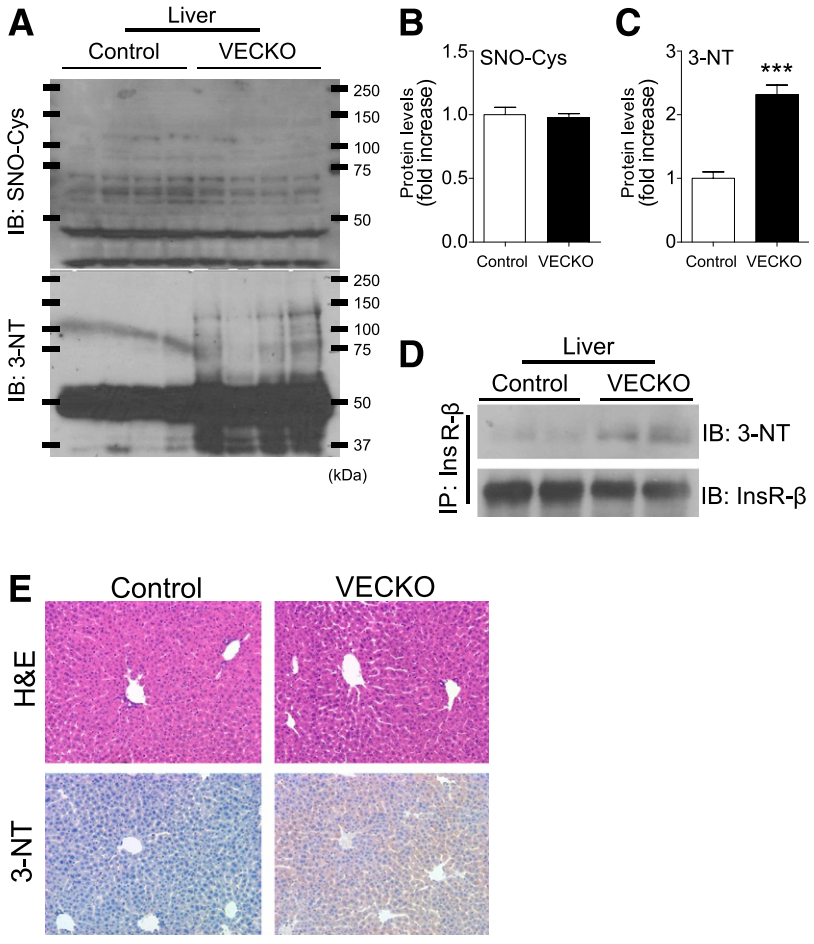

FIG. 5. InsR nitration in liver. *A*: Immunoblots (IB) and quantification of *S*-nitrosylation (SNO-Cys) (*B*) and nitrotyrosine (3-NT) (*C*) in liver from 12-week-old WT and *VECKO* mice ($n = 4$). *D*: Immunoblots of nitrotyrosine in liver tissue after immunoprecipitation with InsR. *E*: Representative photographs of hematoxylin-eosin (H&E) and immunostaining of nitrotyrosine in liver sections. (A high-quality color representation of this figure is available in the online issue.)

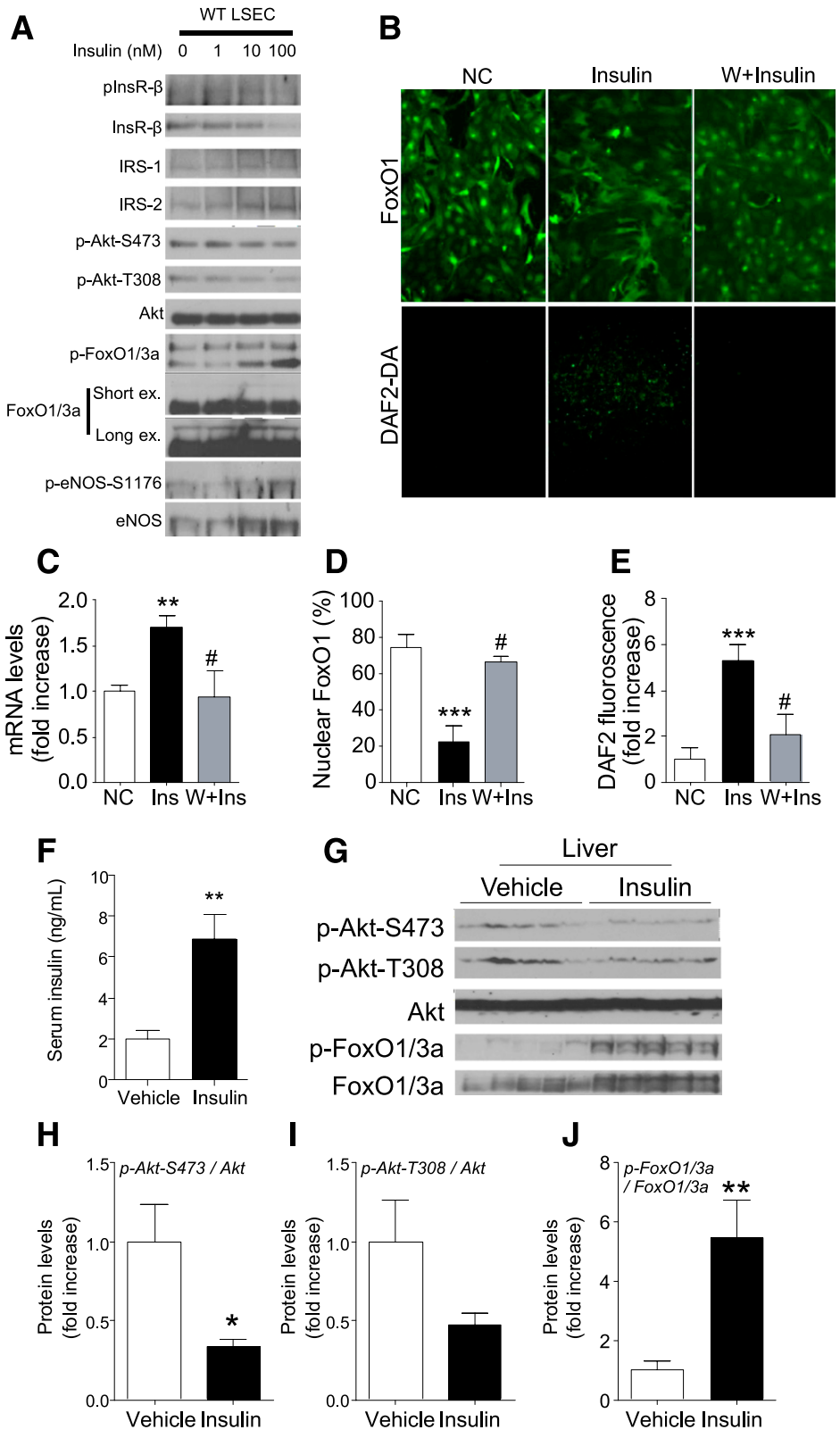

FIG. 6. Insulin signaling and eNos expression after chronic hyperinsulinemia in LSECs. Immunoblots of insulin (Ins) signaling (*A*) and FoxO1 localization (×100) and NO production (×40) (*B*) visualized by DAF-2 DA (DAF2-DA) in cultured WT LSECs treated with insulin (100 nmol/L) for 24 h with or without pretreatment of Wortmannin (W) (20 μmol/L). Quantification of *Nos3* gene expression (*C*), nuclear FoxO1 (*D*), and NO production (*E*) after 24-h insulin treatment (n = 4–5). Serum insulin levels (*F*), immunoblots (*G*), and quantification of insulin signaling (*H–J*) in liver of C57Bl6 mice infused with vehicle or insulin (0.1 units/day) for 72 h (n = 5). NC, nonstimulated control; ex, exposure. *P < 0.05, **P < 0.01, ***P < 0.001 vs. NC or vehicle; #P < 0.05 vs. insulin. (A high-quality color representation of this figure is available in the online issue.)

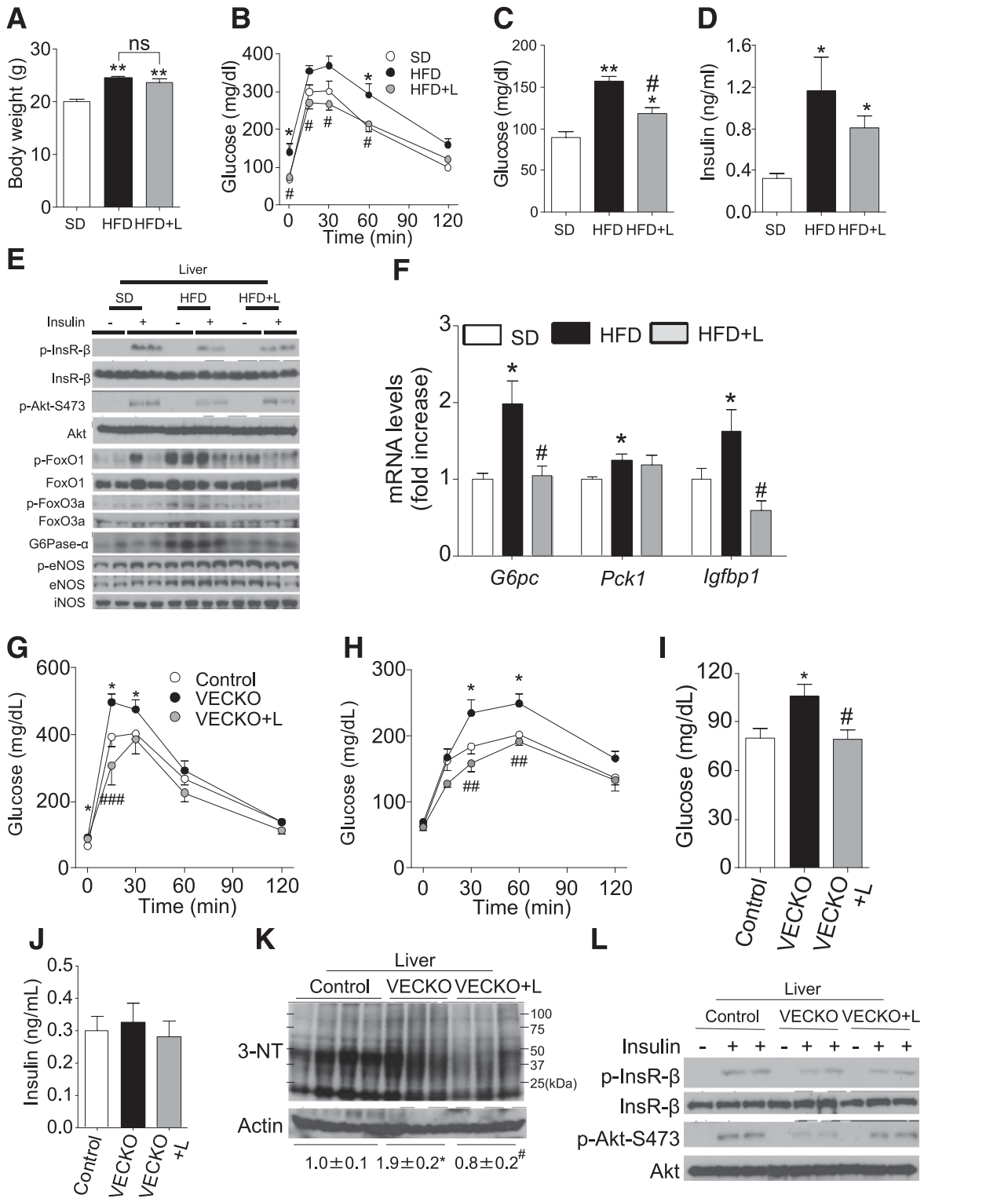

FIG. 7. Pharmacological NO inhibition after SD or short-term HFD. Body weight (*A*), intraperitonal glucose tolerance tests (*B*), glucose (*C*), and insulin (*D*) in 9-week-old mice fed SD or HFD diet for 5 days ($n = 5$). L-NAME (L) administration (2 g/L in drinking water) and fasting were started from 16 h prior to experiments. Representative immunoblots of liver insulin signaling (*E*) and liver gene expression (*F*) in 9-week-old mice fed with SD or HFD for 5 days. We administered insulin after a 16-h fast and collected livers 3 min later ($n = 4$). Intraperitoneal glucose (*G*) and pyruvate (*H*) tolerance tests and glucose (*I*) and insulin (*J*) levels in 12-week-old WT and *VECKO* mice treated with or without L-NAME and fasted for 16 h ($n = 6$–8). L-NAME administration (2 g/L in drinking water) and fasting were started from 16 h prior to experiments. Immunoblots of liver nitrotyrosine (3-NT) (*K*) and insulin signaling (*L*) in 15-week-old WT and *VECKO* mice treated with or without L-NAME (2 g/L in drinking water) with drinking water for 16 h ($n = 3$–4). Livers were collected from 16-h fast mice after 3 min of injection of insulin (Ins) (5 mU/g body wt) or PBS. *$P < 0.05$, **$P < 0.01$ vs. SD or WT. #$P < 0.05$, ##$P < 0.01$, ###$P < 0.001$ vs. HFD or *VECKO*. G6Pase-α, glucose-6-phosphatase-α.

Supplementary Fig. 7*A–E*). In addition, liver p- and total-eNOS expression increased in HFD mice (Fig. 7*E* and Supplementary Fig. 7). L-NAME treatment reversed these findings, increasing Akt phosphorylation and decreasing FoxO phosphorylation; as a result, L-NAME treatment also restored *G6pc* and *Igfbp1* levels to normal (Fig. 7*F*). In contrast, iNOS inhibitor 1400 W did not reverse glucose intolerance in 5-day HFD mice, suggesting that eNOS, rather than iNOS, is the main contributor to the development of glucose intolerance (data not shown). It should be observed that L-NAME treatment was only effective after a short course of HFD (5 days) but not in chronically (15–18 weeks) HFD-fed control (Supplementary Fig. 8*A–C*) or *VECKO* mice (Supplementary Fig. 8*D–K*).

Finally, we determined whether eNos-derived NO overproduction was responsible for the development of hepatic insulin resistance in *VECKO* mice. To this end, we examined hepatic insulin signaling of *VECKO* mice after L-NAME treatment. L-NAME improved glucose tolerance and pyruvate tolerance in *VECKO* mice (Fig. 7*G* and *H*). It also improved fasting hyperglycemia (Fig. 7*I*) and hypercholesterolemia (Supplementary Fig. 6*D*) in *VECKO* mice. Fasting insulin levels were not affected by L-NAME treatment (Fig. 7*J*). Finally, liver protein nitration decreased and insulin signaling improved in *VECKO* mice treated with L-NAME (Fig. 7*K* and *L*). These data are consistent with a causative role of eNos-derived NO in the pathogenesis of hepatic insulin resistance in *VECKO* mice.

DISCUSSION

The current study demonstrates that constitutive insulin signaling in EC—as might be expected to ensue from hyperinsulinemia—affects hepatic insulin action in an indirect manner through NO overproduction in LSECs that leads to tyrosine nitration of InsRs. This, in turn, impairs insulin's ability to restrain expression of glucose production genes, leading to hepatic insulin resistance. Consistent with our findings, a recent report also demonstrated that EC-specific eNOS overexpression in mice was associated with glucose intolerance, although the authors did not investigate the liver phenotype in this model (31). We use mice lacking the three FoxOs in ECs (20) to demonstrate a causative role of the eNos pathway in this process. This turn of events can be reversed by administering L-NAME, providing proof of principle that eNos inhibition in liver has therapeutic benefits in the early stages of insulin resistance. The model arising from these data is that hyperinsulinemia-induced NO overproduction plays an early role in the development of hepatic insulin resistance.

Paracrine role of NO released by LSECs. While mechanistically attractive, the hypothesis that paracrine communication between parenchymal and nonparenchymal cells can cause hepatic insulin resistance finds only sparse support in the literature. Aside from reports that prostaglandins in conditioned medium of cultured nonparenchymal cells increase glycogenolysis in rat hepatocytes (32), there is no prior evidence for a physiological role of LSECs in hepatic glucose metabolism. It also was not obvious, prior to this study, that increased insulin signaling in LSECs, as opposed to decreased insulin signaling, adversely affected hepatic insulin sensitivity.

Our findings highlight the dual nature of NO generated in response to insulin in vascular ECs. In the aorta, constitutive activation of eNos expression and Ser1176 phosphorylation is associated with improved endothelial health and prevents atherosclerosis in Western diet-fed $Ldlr^{-/-}$ mice (20). Conversely, we now show that increased hepatic NO generation predisposes to insulin resistance. This tissue-specific role of eNos-derived NO is not unprecedented. Caveolin1 inhibits NO production by binding to eNos (33). As in $Ldlr^{-/-}$*;VECKO* mice, genetic ablation of *Cav1* on the $Apoe^{-/-}$ background reduces atherosclerosis and increases eNos-dependent NO in ECs (34). But in the lung, *Cav1* knockout increases eNos and induces pulmonary hypertension through tyrosine nitration–dependent impairment of protein kinase G activity (35). These observations suggest that the pathophysiological relevance of persistent eNos-dependent NO production varies from tissue to tissue.

There are no precedents, however, for this type of paracrine regulation of insulin signaling by endothelial NO in the context of an otherwise insulin-sensitive mouse on a normal diet. Consistent with the notion that the LSEC-dependent mechanisms play an initiating role in the metabolic syndrome, we find that treatment of established insulin resistance, e.g., in mice fed an HFD for 18 weeks, is no longer reversible by NO inhibition, suggesting that other events (lipotoxicity, inflammation, and metabolic inflexibility) account for the progression of insulin resistance. Likewise, it is interesting to note that *VECKO* mice only exhibit insulin resistance on a regular diet but not on the more metabolically challenging HFD or Western-type diet on the $Ldlr^{-/-}$ background (20), suggesting that other factors trump the role of LSECs in the transition from early to advanced insulin resistance. For instance, iNos produced in response to inflammatory cytokines in the obese state can generate significantly more NO than eNos (36–38).

Tyrosine nitration and insulin resistance. Tyrosine nitration is a biomarker of nitrosative stress in pathological conditions, including insulin resistance (39–41). In insulin signaling, it has been reported that tyrosine residues of InsR, Irs1 and -2, and Akt can be nitrated (28,42), altering their function by preventing phosphorylation (43,44). In contrast, we show that insulin sensitivity in adipose tissue and skeletal muscle was unaffected, possibly due to differences in tissue content of ECs and eNOS-derived NO or tissue sensitivity to NO. We suggest that the eNos-dependent NO overproduction promotes protein nitration, impairing hepatic insulin signaling.

Additional mechanisms of endothelial/hepatocyte interaction. We focused our studies on the role of eNos-derived NO in insulin InsR signaling. But there are likely to be additional mechanisms that mediate endothelial/hepatocyte interactions, potentially affecting insulin sensitivity. In line with our observations, previous studies have suggested that NO can inhibit glycogen synthesis and glucose uptake in liver, possibly independent of insulin signaling. Thus, the NO donor, *S*-nitroso-*N*-acetylpenicillamine, can impair glycogen synthase, decreasing glycogen synthesis (45). NO infusion increases glucose output in the perfused rat liver by stimulating glycogenolysis (46,47). Consistent with our results, portal delivery of NO enhances hepatic glucose output (47,48)—an effect that is blocked by inhibition of guanylate cyclase (48). Our findings suggest that local—as opposed to systemic—NO production can explain these effects.

Conclusions. Based on the present data, we propose the following model for the progression of insulin resistance: In response to a decrease in insulin-dependent glucose uptake in skeletal muscle, insulin levels increase, resulting in hyperinsulinemia. Sustained hyperinsulinemia inactivates

insulin signaling in LSECs, causes FoxO nuclear exclusion, increases NO production in the liver, and impairs insulin's ability to suppress glucose production. Hence, we propose that lowering hyperinsulinemia should be a focus of treatment in the early phases of the metabolic syndrome. NO inhibition in liver could have beneficial effects in preventing insulin resistance.

ACKNOWLEDGMENTS

K.T. is the recipient of a postdoctoral fellowship for research abroad from the Japan Society for the Promotion of Science. This work was supported by National Institutes of Health grants HL87123, DK58282, and DK63608 (Columbia University Diabetes Research Center).

No potential conflicts of interest relevant to this article were reported.

K.T. and D.A. designed and performed experiments, analyzed data, and wrote the manuscript. D.A. is the guarantor of this work and, as such, had full access to all the data in the study and, as such, takes responsibility for the integrity of the data and the accuracy of the data analysis.

The authors thank members of the Accili laboratory for constructive advice and discussion of data.

REFERENCES

1. Accili D. Lilly lecture 2003: the struggle for mastery in insulin action: from triumvirate to republic. Diabetes 2004;53:1633–1642
2. Weyer C, Hanson RL, Tataranni PA, Bogardus C, Pratley RE. A high fasting plasma insulin concentration predicts type 2 diabetes independent of insulin resistance: evidence for a pathogenic role of relative hyperinsulinemia. Diabetes 2000;49:2094–2101
3. Taylor SI. Lilly Lecture: molecular mechanisms of insulin resistance. Lessons from patients with mutations in the insulin-receptor gene. Diabetes 1992;41:1473–1490
4. Gavin JR 3rd, Roth J, Neville DM Jr, de Meyts P, Buell DN. Insulin-dependent regulation of insulin receptor concentrations: a direct demonstration in cell culture. Proc Natl Acad Sci USA 1974;71:84–88
5. Rizza RA, Mandarino LJ, Gerich JE. Dose-response characteristics for effects of insulin on production and utilization of glucose in man. Am J Physiol 1981;240:E630–E639
6. Kolterman OG, Gray RS, Griffin J, et al. Receptor and postreceptor defects contribute to the insulin resistance in noninsulin-dependent diabetes mellitus. J Clin Invest 1981;68:957–969
7. Poy MN, Yang Y, Rezaei K, et al. CEACAM1 regulates insulin clearance in liver. Nat Genet 2002;30:270–276
8. Sindelar DK, Balcom JH, Chu CA, Neal DW, Cherrington AD. A comparison of the effects of selective increases in peripheral or portal insulin on hepatic glucose production in the conscious dog. Diabetes 1996;45:1594–1604
9. Lin HV, Plum L, Ono H, et al. Divergent regulation of energy expenditure and hepatic glucose production by insulin receptor in agouti-related protein and POMC neurons. Diabetes 2010;59:337–346
10. Michael MD, Kulkarni RN, Postic C, et al. Loss of insulin signaling in hepatocytes leads to severe insulin resistance and progressive hepatic dysfunction. Mol Cell 2000;6:87–97
11. Kono T, Barham FW. The relationship between the insulin-binding capacity of fat cells and the cellular response to insulin. Studies with intact and trypsin-treated fat cells. J Biol Chem 1971;246:6210–6216
12. Kubota T, Kubota N, Kumagai H, et al. Impaired insulin signaling in endothelial cells reduces insulin-induced glucose uptake by skeletal muscle. Cell Metab 2011;13:294–307
13. Kondo T, Vicent D, Suzuma K, et al. Knockout of insulin and IGF-1 receptors on vascular endothelial cells protects against retinal neovascularization. J Clin Invest 2003;111:1835–1842
14. Vicent D, Ilany J, Kondo T, et al. The role of endothelial insulin signaling in the regulation of vascular tone and insulin resistance. J Clin Invest 2003;111:1373–1380
15. Rask-Madsen C, Li Q, Freund B, et al. Loss of insulin signaling in vascular endothelial cells accelerates atherosclerosis in apolipoprotein E null mice. Cell Metab 2010;11:379–389
16. Barrett EJ, Wang H, Upchurch CT, Liu Z. Insulin regulates its own delivery to skeletal muscle by feed-forward actions on the vasculature. Am J Physiol Endocrinol Metab 2011;301:E252–E263
17. Bergman RN. Orchestration of glucose homeostasis: from a small acorn to the California oak. Diabetes 2007;56:1489–1501
18. Chisalita SI, Arnqvist HJ. Insulin-like growth factor I receptors are more abundant than insulin receptors in human micro- and macrovascular endothelial cells. Am J Physiol Endocrinol Metab 2004;286:E896–E901
19. Treadway JL, Morrison BD, Soos MA, et al. Transdominant inhibition of tyrosine kinase activity in mutant insulin/insulin-like growth factor I hybrid receptors. Proc Natl Acad Sci USA 1991;88:214–218
20. Tsuchiya K, Tanaka J, Shuiqing Y, et al. FoxOs integrate pleiotropic actions of insulin in vascular endothelium to protect mice from atherosclerosis. Cell Metab 2012;15:372–381
21. Nakae J, Biggs WH 3rd, Kitamura T, et al. Regulation of insulin action and pancreatic beta-cell function by mutated alleles of the gene encoding forkhead transcription factor Foxo1. Nat Genet 2002;32:245–253
22. Matsumoto M, Pocai A, Rossetti L, Depinho RA, Accili D. Impaired regulation of hepatic glucose production in mice lacking the forkhead transcription factor Foxo1 in liver. Cell Metab 2007;6:208–216
23. Kitamura YI, Kitamura T, Kruse JP, et al. FoxO1 protects against pancreatic beta cell failure through NeuroD and MafA induction. Cell Metab 2005;2:153–163
24. Fulton D, Gratton JP, McCabe TJ, et al. Regulation of endothelium-derived nitric oxide production by the protein kinase Akt. Nature 1999;399:597–601
25. Potente M, Urbich C, Sasaki KI, et al. Involvement of Foxo transcription factors in angiogenesis and postnatal neovascularization. J Clin Invest 2005;115:2382–2392
26. Tanaka J, Qiang L, Banks AS, et al. Foxo1 links hyperglycemia to LDL oxidation and endothelial nitric oxide synthase dysfunction in vascular endothelial cells. Diabetes 2009;58:2344–2354
27. Radi R. Nitric oxide, oxidants, and protein tyrosine nitration. Proc Natl Acad Sci USA 2004;101:4003–4008
28. Charbonneau A, Marette A. Inducible nitric oxide synthase induction underlies lipid-induced hepatic insulin resistance in mice: potential role of tyrosine nitration of insulin signaling proteins. Diabetes 2010;59:861–871
29. Gonzalez E, Flier E, Molle D, Accili D, McGraw TE. Hyperinsulinemia leads to uncoupled insulin regulation of the GLUT4 glucose transporter and the FoxO1 transcription factor. Proc Natl Acad Sci USA 2011;108:10162–10167
30. Surwit RS, Kuhn CM, Cochrane C, McCubbin JA, Feinglos MN. Diet-induced type II diabetes in C57BL/6J mice. Diabetes 1988;37:1163–1167
31. Sansbury BE, Cummins TD, Tang Y, et al. Overexpression of endothelial nitric oxide synthase prevents diet-induced obesity and regulates adipocyte phenotype. Circ Res 2012;111:1176–1189
32. Casteleijn E, Kuiper J, van Rooij HC, Kamps JA, Koster JF, van Berkel TJ. Hormonal control of glycogenolysis in parenchymal liver cells by Kupffer and endothelial liver cells. J Biol Chem 1988;263:2699–2703
33. Michel JB, Feron O, Sacks D, Michel T. Reciprocal regulation of endothelial nitric-oxide synthase by Ca2+-calmodulin and caveolin. J Biol Chem 1997;272:15583–15586
34. Fernández-Hernando C, Yu J, Suárez Y, et al. Genetic evidence supporting a critical role of endothelial caveolin-1 during the progression of atherosclerosis. Cell Metab 2009;10:48–54
35. Frank PG, Lee H, Park DS, Tandon NN, Scherer PE, Lisanti MP. Genetic ablation of caveolin-1 confers protection against atherosclerosis. Arterioscler Thromb Vasc Biol 2004;24:98–105
36. Noronha BT, Li JM, Wheatcroft SB, Shah AM, Kearney MT. Inducible nitric oxide synthase has divergent effects on vascular and metabolic function in obesity. Diabetes 2005;54:1082–1089
37. Perreault M, Marette A. Targeted disruption of inducible nitric oxide synthase protects against obesity-linked insulin resistance in muscle. Nat Med 2001;7:1138–1143
38. Shinozaki S, Choi CS, Shimizu N, et al. Liver-specific inducible nitric-oxide synthase expression is sufficient to cause hepatic insulin resistance and mild hyperglycemia in mice. J Biol Chem 2011;286:34959–34975
39. Ischiropoulos H. Protein tyrosine nitration—an update. Arch Biochem Biophys 2009;484:117–121
40. Kaneki M, Shimizu N, Yamada D, Chang K. Nitrosative stress and pathogenesis of insulin resistance. Antioxid Redox Signal 2007;9:319–329
41. Fujimoto M, Shimizu N, Kunii K, Martyn JA, Ueki K, Kaneki M. A role for iNOS in fasting hyperglycemia and impaired insulin signaling in the liver of obese diabetic mice. Diabetes 2005;54:1340–1348
42. Nomiyama T, Igarashi Y, Taka H, et al. Reduction of insulin-stimulated glucose uptake by peroxynitrite is concurrent with tyrosine nitration of insulin receptor substrate-1. Biochem Biophys Res Commun 2004;320:639–647

43. Mondoro TH, Shafer BC, Vostal JG. Peroxynitrite-induced tyrosine nitration and phosphorylation in human platelets. Free Radic Biol Med 1997;22:1055–1063
44. Rawlingson A, Shendi K, Greenacre SA, et al. Functional significance of inducible nitric oxide synthase induction and protein nitration in the thermally injured cutaneous microvasculature. Am J Pathol 2003;162:1373–1380
45. Sprangers F, Sauerwein HP, Romijn JA, van Woerkom GM, Meijer AJ. Nitric oxide inhibits glycogen synthesis in isolated rat hepatocytes. Biochem J 1998;330:1045–1049
46. Borgs M, Bollen M, Keppens S, Yap SH, Stalmans W, Vanstapel F. Modulation of basal hepatic glycogenolysis by nitric oxide. Hepatology 1996;23:1564–1571
47. Ming Z, Han C, Lautt WW. Nitric oxide inhibits norepinephrine-induced hepatic vascular responses but potentiates hepatic glucose output. Can J Physiol Pharmacol 2000;78:36–44
48. An Z, Winnick JJ, Farmer B, et al. A soluble guanylate cyclase-dependent mechanism is involved in the regulation of net hepatic glucose uptake by nitric oxide in vivo. Diabetes 2010;59:2999–3007